the plant journal

SEB SOCIETY FOR EXPERIMENTAL BIOLOGY

The Plant Journal (2024) **120,** 1377–1391 doi: 10.1111/tpj.17055

Leaf abaxial and adaxial surfaces differentially affect the interaction of *Botrytis cinerea* across several eudicots

Celine Caseys[1], Anna Jo Muhich[1,2], Josue Vega[1], Maha Ahmed[1], Aleshia Hopper[1], David Kelly[1], Sydney Kim[1], Matisse Madrone[1], Taylor Plaziak[1], Melissa Wang[1] and Daniel J. Kliebenstein[1,2,*]

[1]*Department of Plant Sciences, University of California, Davis, Davis, California, USA, and*

[2]*Plant Biology Graduate Group, University of California, Davis, Davis, California, USA*

Received 9 February 2024; accepted 17 September 2024; published online 4 October 2024.

*For correspondence (e-mail kliebenstein@ucdavis.edu)

SUMMARY

Eudicot plant species have leaves with two surfaces: the lower abaxial and the upper adaxial surface. Each surface varies in a diversity of components and molecular signals, resulting in potentially different degrees of resistance to pathogens. We tested how *Botrytis cinerea*, a necrotroph fungal pathogen, interacts with the two different leaf surfaces across 16 crop species and 20 Arabidopsis genotypes. This showed that the abaxial surface is generally more susceptible to the pathogen than the adaxial surface. In Arabidopsis, the differential lesion area between leaf surfaces was associated with jasmonic acid (JA) and salicylic acid (SA) signaling and differential induction of defense chemistry across the two surfaces. When infecting the adaxial surface, leaves mounted stronger defenses by producing more glucosinolates and camalexin defense compounds, partially explaining the differential susceptibility across surfaces. Testing a collection of 96 *B. cinerea* strains showed the genetic heterogeneity of growth patterns, with a few strains preferring the adaxial surface while most are more virulent on the abaxial surface. Overall, we show that leaf–Botrytis interactions are complex with host-specific, surface-specific, and strain-specific patterns.

Keywords: plant–pathogen interactions, *Botrytis cinerea*, necrotroph fungi, crops, leaf surfaces, defense signaling, plant development.

INTRODUCTION

When pathogens attack, they battle with the plants to establish and grow (Ferreira et al., 2006; Pandey et al., 2016). The pathogens first face constitutive defenses and then likely trigger the plant immune system with various receptors and signaling pathways (Kushalappa et al., 2016; Zipfel, 2008). As such, the outcome of the pathogen attack depends on the combinatorial interplay of the constitutive and induced physical and chemical defenses. However, these defenses further vary independently of the pathogens attack across environmental (Lacchini & Goossens, 2020; Mitreiter & Gigolashvili, 2021), genotypic (Ballhorn et al., 2011; Potts & Hunter, 2021) and developmental (Chung et al., 2008; Kong & Yang, 2023) landscapes.

Developmental variations in plant defenses are beginning to be studied in more detail. For example, age-related resistance is critical in the interactions with diverse pathogens (Hu & Yang, 2019). A key developmental aging process is fruit ripening which alters physical and signaling defenses altering pathogen interactions (Forlani et al., 2019; Petrasch et al., 2019; Silva et al., 2023). In the leaf, spatial gradients along the axis of the leaf blade are linked to differential hormone responses and growth capacity affecting biotrophic fungi such as *Blumeria hordei* (Krasauskas et al., 2023). While developmental transitions are key to plant–pathogen interactions (Hu & Yang, 2019; Kong & Yang, 2023), the impact of a developmental transition across diverse host species on a single pathogen is not typically cataloged using both plant and pathogen genetic variation. Thus, a system in which the same interaction can be systematically studied across plant species is needed to develop a better understanding of how plant development influences host–pathogen interactions. In this work, we are using the generalist pathogen, *Botrytis cinerea*, to begin a systematic assessment of how development influences host interactions both across and within species.

To accomplish this, we focus on the difference between the two surfaces of the angiosperm leaves (Foster, 1936), the abaxial and adaxial leaf surfaces, which have distinct physical properties (Tsukaya, 2014). Studies are beginning to suggest that these leaf surfaces affect the

host–pathogen interaction (Caires et al., 2014). In hybrids of *Lilium auratum* and *L. speciosum* (oriental lilies), microscopy observations revealed *Botrytis elliptica* failed to invade epidermal cells on the adaxial side while successfully invading from the abaxial (Hsieh et al., 2001). Similarly, in *Vicia faba* (faba bean), it was shown that infection from both the specialist *Botrytis fabae* and the generalist *B. cinerea* developed larger lesions on the abaxial than the adaxial surface (Hashim et al., 1997). While these studies suggest that developmental patterns between leaf surfaces on monocots and dicots can influence host–pathogen interactions, how this phenomenon and the mechanisms involved translate across diverse host plants remains unknown.

Based on leaf physiological knowledge, environmental (Berens et al., 2019; Liu et al., 2020; Ritpitakphong et al., 2016; Schäfer et al., 2023), physical (Calo et al., 2006; Mafia et al., 2009), chemical (Aragón et al., 2017; Fernández et al., 2017; Ziv et al., 2018), and/or hormonal (Kazan & Manners, 2009; Kidner & Timmermans, 2010; Liu et al., 2012) properties could explain the developmental effect of the leaf surfaces on host–pathogen interactions. First, abaxial and adaxial leaf surfaces present different cell densities. The adaxial surface is composed of the upper epidermis covering the dense mesophyll (Zuch et al., 2022), while the abaxial surface is composed of the lower epidermis covering the loosely packed spongy mesophyll (Whitewoods, 2021). The leaf surfaces can also vary in the presence and composition of the thick and rigid chemical barrier, the cuticle (Aragón et al., 2017; Fernández et al., 2017; Ziv et al., 2018). These variations in cell density and surface chemistry might impact the hyphal turgor pressure (Lew, 2019) necessary to invade the leaf. Alternatively, the pathogen could use stomata penetration (Meddya et al., 2023), entering these pores predominantly positioned on the abaxial surface. Trichomes can also provide additional physical barriers preventing fungal spores from reaching the leaf surface (Kim, 2019). However, later in the infection process, trichomes can anchor growing fungal hyphae close to the leaf surface and contribute to the pathogen's propagation (Calo et al., 2006).

In addition to these surface parameters, different signaling processes and/or outputs could alter host–pathogen interactions. In leaf bifacial development, auxin signaling plays a major role in controlling complex networks of regulatory genes (Kidner & Timmermans, 2010; Liu et al., 2012). The HD-ZIPIII family determines the adaxial, while the KANADI and auxin response factor (ARF) families determine the abaxial side. The YABBY family is another important class of transcription factor (TF) involved in both abaxial development and stress responses (Zhang et al., 2020). In complement, crosstalk between auxin and the defense-associated hormones salicylic acid (SA) and jasmonic acid (JA) is described (Kazan & Manners, 2009). These signaling variations generate expression profiles with hundreds of genes differentially expressed between the leaf surfaces (Tian et al., 2019). Those differential expression patterns are visible in the defense chemistry with abaxial and adaxial epidermal cells producing differing amounts of metabolites (Tenorio Berrío et al., 2022). In glucosinolates, a family of defense compounds well-described from signaling (Mitreiter & Gigolashvili, 2021) to their impact on plant–pathogen interaction (Plaszkó et al., 2022), a 10-fold differential concentration was observed in Arabidopsis across the leaf, with more abundance on the abaxial than the adaxial surface (Shroff et al., 2015).

To test how the leaf surfaces influence host–pathogen interactions both across and within plant species, we used *B. cinerea* (gray mold, Botrytis blight, Botrytis thereafter). This generalist fungal pathogen is an endemic pathogen that infects more than a thousand plant species (Fillinger & Elad, 2016; Singh et al., 2023). Botrytis broad-host pathogenic ability relies on its polygenic genetic architectures and a wide diversity of specific mechanisms (Bi et al., 2022; Pink et al., 2022; Singh et al., 2023). Botrytis penetration of the host's cells can be opportunistic through stomata and wounds or intentional through penetration of the epidermis with infection cushions (Choquer et al., 2021; Hsieh et al., 2001). In addition, Botrytis uses a diversity of additional mechanisms to facilitate virulence including cell wall degrading enzymes (Bi et al., 2022), toxins (da Silva et al., 2023), and small RNAs manipulating the host's transcriptome (Weiberg et al., 2013). Botrytis' cell-death-inducing proteins (Bi et al., 2022; Veloso & van Kan, 2018) further contribute to toxic levels of reactive oxygen species (Siegmund & Viefhues, 2016), lesion expansion, and tissue maceration. It is currently unclear how this cell death may or may not relate to hypersensitive responses (Govrin & Levine, 2000; Jeblick et al., 2023) induced by biotrophic pathogens via NBS-LRRs (Feechan et al., 2015). These diverse mechanisms are redundant (Leisen et al., 2022) and build additively based on standing genetic variation (Atwell et al., 2018; Mercier et al., 2021). This genetic diversity allows a population of Botrytis strains to be a highly useful tool in querying if the effects of leaf development vary across diverse strains and how this may be influenced by the variation between host plants.

To assess how developmental patterns between leaf surfaces influence Botrytis interactions, we first tested 16 species from eight different plant families (Figure 1a) with diverse natural histories. These eight families are sampled from the caryophyllales in the basal core eudicots to asterids and rosids (Soltis & Soltis, 2004). As physical and chemical defenses and also defense signaling were shaped by the environment, herbivore, and pathogen pressures across the evolutionary timescale (Berens et al., 2017; Endara et al., 2023), those species constitute a sampling of defensive strategies existing in the eudicots while focusing

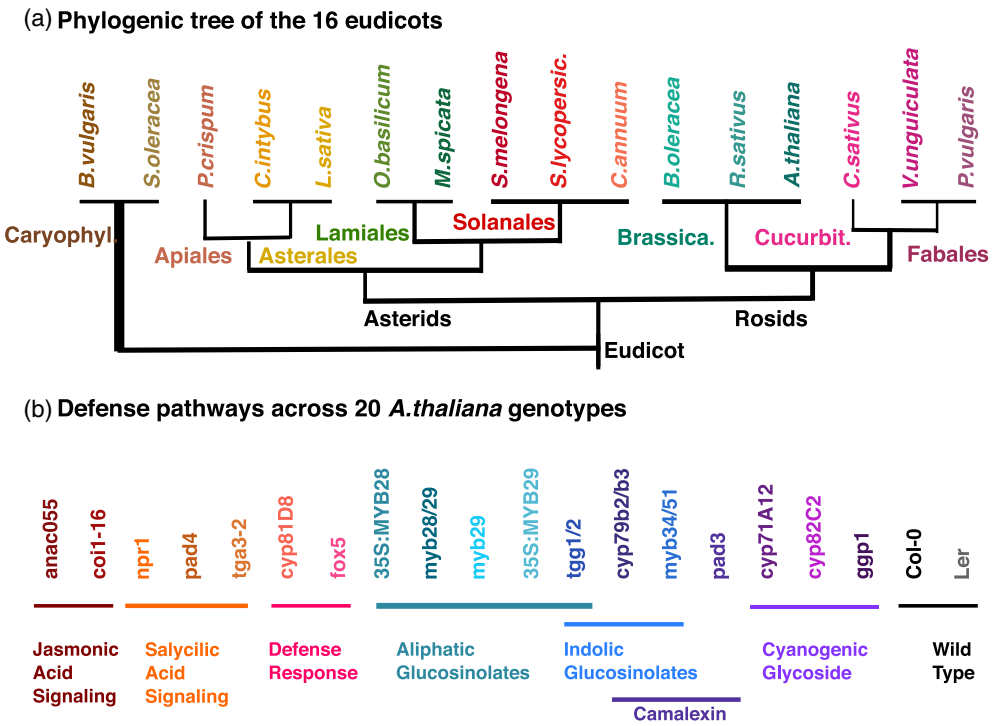

Figure 1. (a) Phylogeny of the 16 eudicot species (Table S1) used to test how the leaf surfaces influence host–pathogen interactions across species. The families and orders are indicated on the branches.
(b) The 20 Arabidopsis genotypes used to test how leaf surfaces change the interaction with Botrytis within a species. The genotypes are grouped (horizontal lines) and colored by their defense pathways (Table S2).

on crops of economical value. To test how the effect of the leaf surfaces varies across genotypes within a host species, we infected 20 *A. thaliana* genotypes (Figure 1b). Those genotypes included SA and JA signaling mutants that control over the chemical defense variation in addition to TFs and enzymes along the pathways (Mitreiter & Gigolashvili, 2021). Finally, to assess how the diversity in the pathogen interacts with developmental patterns between leaf surfaces, we infected 96 Botrytis strains on a single host genotype. This provided an analysis of how abaxial/adaxial leaf surface variation influences the host–Botrytis interaction across diverse host species, host genotypes, and pathogen genotypes providing an initial investigation into the conditionality of this phenomena.

RESULTS

The leaf physical properties do not explain the surface effect across eudicot hosts

To test whether differences in the adaxial and abaxial leaf surfaces influence Botrytis interactions across the eudicots, we infected 16 species with 10 strains of Botrytis (Table S3). The plant species were chosen from the caryophyllales, rosids, and asterids (Figure 1a) and sample a diversity of leaf thickness, stomata sizes, and densities (Figure 2a) across the leaf surfaces (Table S1). For example, measuring stomatal density across the species confirmed the expected relationship where the abaxial surface has more stomata (range 215–1052 stomata/mm^2, Table S1) than the adaxial surface (range: 0–556 stomata/mm^2, Table S1). However, this ratio is highly variable with some species like *A. thaliana*, and *Ocimum basilicum* (basil) having a small difference between the surfaces, while some like *Phaseolus vulgaris* (bean), *Capsicum annuum* (pepper), and *Mentha spicata* (mint) have near presence/absence variation across the surfaces (Figure 2a).

Infecting Botrytis on the leaves of all species showed an overall trend for larger lesion areas on the abaxial than adaxial surfaces (Figure 2b; Table S1; Figure S1a). The larger abaxial lesions were measured on all species except *Beta vulgaris* (chard) and *Lactuca sativa* (lettuce) (Table S1; Figure 2b). This trend was statistically significant in six species (Figure 2b; Figure S1b) spread across the eudicot phylogeny: *A. thaliana*, *Vigna unguiculata* (cowpea), *Solanum melongena* (eggplant), *Brassica oleracea* (kale), *Petroselinum crispum* (parsley), and *Spinacia oleracea* (spinach). Overall plant susceptibility across the eudicots did not play a role in the surface differential (Figures S1a and S2a). Similarly, the lesion area differential between the adaxial and abaxial leaf surfaces had no correlation to

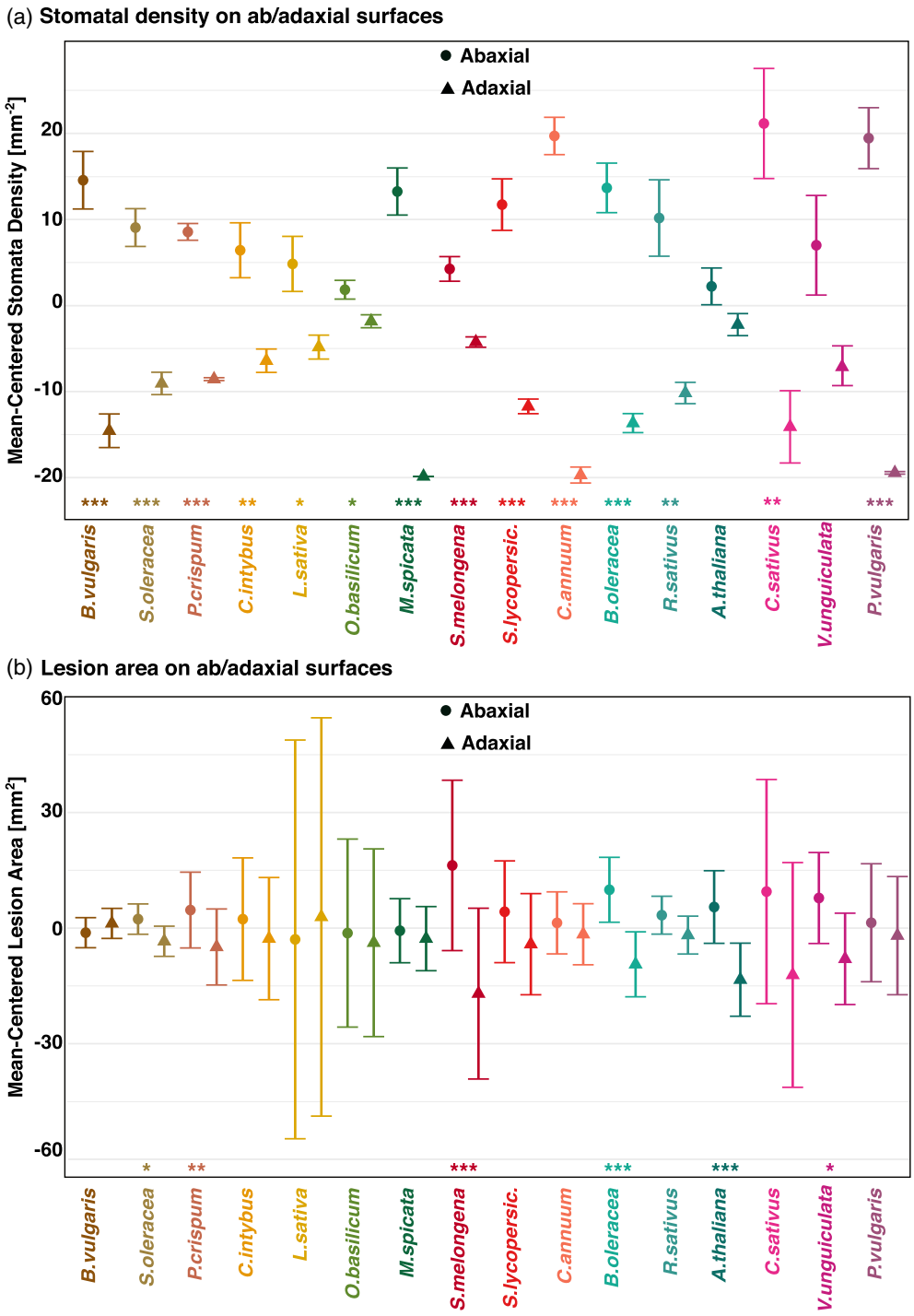

Figure 2. The susceptibility of leaf surfaces to *B. cinerea* across the eudicot does not depend on stomata density and vary across hosts.
(a) Mean-centered abaxial/adaxial stomatal density (stomata/mm^2; Table S1) and standard error bars (n = 6).
(b) Mean-centered lesion area [mm^2] (Table S1) on abaxial/adaxial leaf surfaces and standard error bars (n = 10 strains*6 replicates) measured at 72 HPI.
(a, b) Given the large variation among the species in terms of resistance (Figure S1a), the data were centered by subtraction of mean of each species to parse the leaf surface and species effects. Circles represent the lower abaxial surface, while up-pointing triangles represent the upper adaxial surface. Level of significance of surface effect within species: ***P < 0.001, **P < 0.01, and *P < 0.05.

stomatal density on the surfaces nor leaf thickness (Figure S2b–f). This suggests that the effect of variation between leaf surfaces on host–Botrytis interactions is variable across the eudicots and is not predominantly driven by these measured physical aspects like stomatal density or leaf thickness variation.

Defense signaling and chemical defenses both influence the surface effect

To test how variation between leaf surfaces changes within a host species, we utilized the extensive availability of mutants in *A. thaliana*. We infected 18 mutants (Table S2) and Ler as an additional accession (Figure 1b). These mutants allowed testing if methionine/tryptophan-derived defense chemistry and/or defense signaling affect Botrytis lesion formation when infected on different leaf surfaces. The mutants were infected with the 10 Botrytis strains that sample the range of virulence on Arabidopsis (Table S3). The level of significance of the surface effect in Col-0 (Figures 2 and 3) depended on the set of 10 Botrytis strains tested (Table S3).

Measuring the lesion area on the leaf surfaces of these Arabidopsis genotypes with various susceptibilities revealed three patterns. First, some mutants had limited or inversed surface differentials compared to WT; for example, the size of the lesions on both surfaces was more equal than in WT. This pattern was observed for *cyp81D8*, the double knockout mutant of *myb28/29*, the single knockout of myb29, the *35S:MYB28* overexpression line, and the *35S:MYB29* overexpression line (although *35S*:MYB29 had a strong differential at 72 h and then plateaued, Figure 3b). In the second observed pattern, the mutations amplified the surface effect indicated as having a significantly larger lesion area on abaxial than adaxial surface without increasing the overall plant susceptibility (Figure 3a). This pattern was observed in *npr1* and *pad4* involved in salicylic acid signaling defense responses. It was also observed *in tgg1/2*, the double mutant for the two myrosinase enzymes that convert glucosinolates into toxic isothiocyanates. The mutants in *cyp71a12* and *cyp82c2* involved in the biosynthesis of 4-hydroxy indole3-carbonyl nitrile, a potential indole-cyanogenic glycoside phytoalexin, also showed this pattern. In the final pattern, the mutants lead to both an increased surface effect and of the overall plant susceptibility (larger lesion area compared to Col-0, Figure 3a). This pattern was observed for *coi1-16* involved in jasmonic acid signaling and *tga3* a TF involved in salicylic acid signaling defense response. The double mutants *myb34/51*, *cyp79b2/cyp79b3*, and the *pad3* single mutant, all abolishing camalexin production also showed this pattern. While the surface differential in lesion area largely increases linearly in time as with Col-0, some mutant lines have different temporal trajectories including the biosynthetic mutants *cyp79b2b3*, *cyp81D8*, and 35S:*MYB29* (Figure 3b). This suggests that the differential surface effect is affected by both signaling and defense metabolism pathways in Arabidopsis–Botrytis interactions.

To test whether Botrytis' early growth, such as observed in cyp79b2/b3 (Figure 3b), could result from different infection strategies on the leaf surfaces (infection cushion or stomata), we infected, stained, and microscopically observed Botrytis hyphae on both leaf surfaces across a time course between 24 and 72 HPI. We also visualized infected leaves from Col-0, *myb28/29*, *35S:MYB28*, *tgg1/2*, *myb34/51*, and *pad3* to assess a range of plant susceptibility and surface differential effects (Figure 3). While there was variation in hyphal density linked to a faster growth rate on genotypes producing no camalexin (cyp79b2/b3, pad3), we did not observe variation in tissue penetration strategies. Across all genotypes and leaf surfaces, we consistently observed that the infection cushions, a multicellular structure specialized in breaching the host tissue through mechanical and chemical actions, directly target the area of the pavement cells (Figure S3). This suggests that the base infection strategy was similar across all Arabidopsis samples including abaxial and adaxial leaf surfaces, genotypes, and times. These observations suggested that the differential lesion area between leaf surfaces in Arabidopsis is not associated with a dramatic shift in Botrytis tissue penetration strategy.

Differential induction of glucosinolates across leaf surfaces

A core defense mechanism of Arabidopsis against Botrytis is specialized metabolites like camalexin and glucosinolates (Buxdorf et al., 2013; Ferrari et al., 2003) that are controlled by SA and JA signaling pathways (Mitreiter & Gigolashvili, 2021). To test how these metabolites may differentially influence Botrytis–host leaf surface interactions, ten Botrytis strains were infected on the abaxial and adaxial surface of six defense metabolite mutants (*35S:MYB28*, *myb28/29*, *tgg1/2*, *myb34/51*, *cyp79b2/b3*, and *pad3*) and their wild-type genotype Col-0. These metabolites are known for their role in plant defense and can be directly measured by HPLC (Figure S4). To estimate how the variation between leaf surfaces related to Botrytis virulence and/or plant chemical defenses, we used linear modeling to parse their effects. Across mutants, the variation in camalexin, indolic, and aliphatic GSLs explained respectively 15.7%, 3.2%, and 1.1% of the variance in lesion area (Figure S5). Linear regressions further confirmed that the concentration of camalexin was negatively correlated to lesion area in *35S:MYB28*, *myb28/29*, *tgg1/2*, *and* Col-0 (Figure S6). The concentration of aliphatic GSLs was negatively correlated to the lesion area in *myb34/51*, *cyp79b2/b3*, and Col-0 (Figure S7), while I3M was negatively correlated to the lesion area in *tgg1/2*, *pad3*, and Col-0 (Figure S8). These results confirmed the defensive role of camalexin and glucosinolates against Botrytis. Moving to the leaf surface effect, the effect of infecting the abaxial and adaxial leaf surfaces was smaller than the effect of chemical defenses, explaining 2.5% of the total variance in lesion area. However, there was a significant interaction leaf surface interaction identified with camalexin (Figure S5).

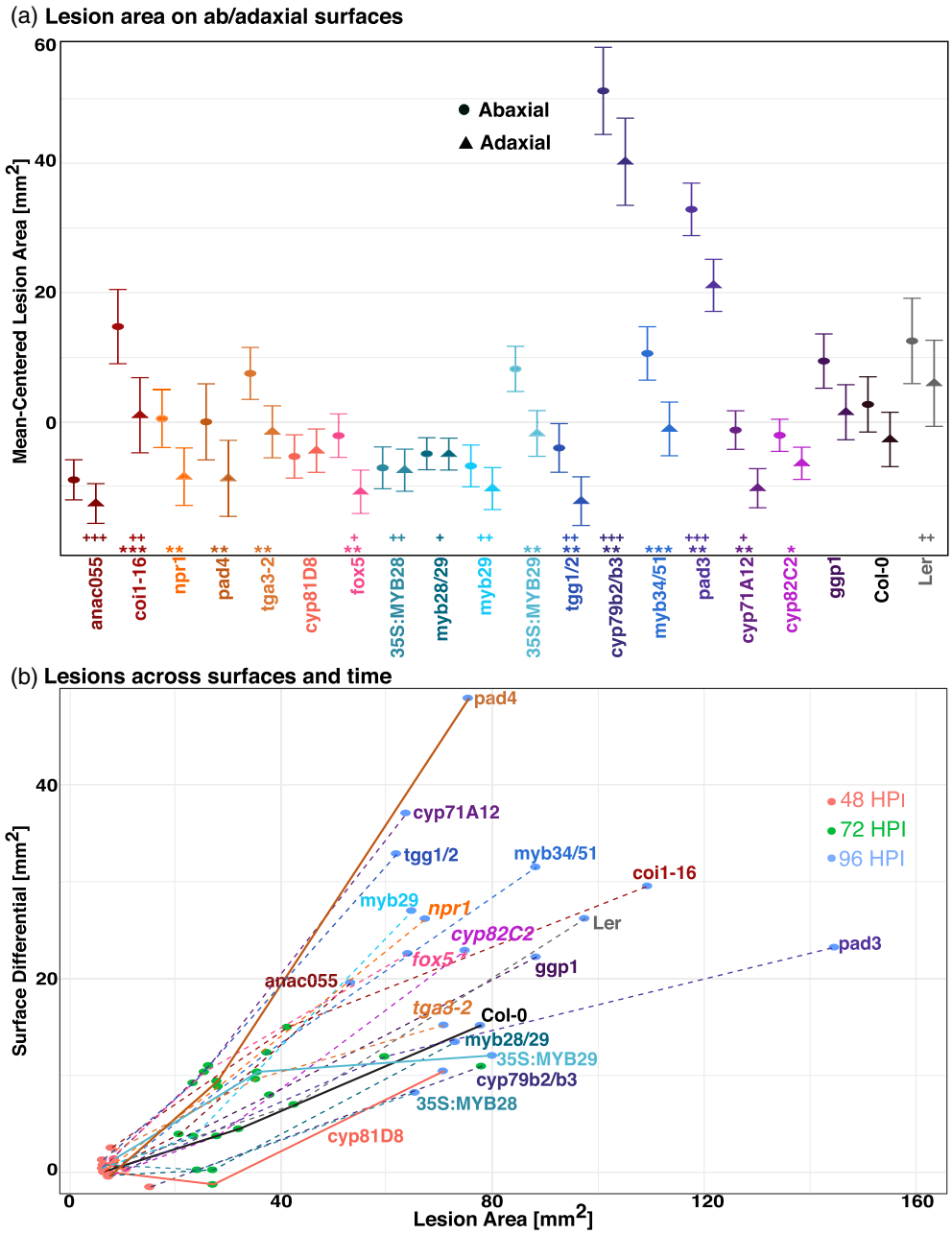

Figure 3. The susceptibility of *A. thaliana* leaf surfaces to *B. cinerea* varies with defense signaling and chemistry.
(a) Mean-centered lesion area [mm^2] and standard error bars (n = 10 strains*4 replicates) as modeled at 72 HPI on each surface. To parse the effects of the background accession, lesion areas were centered by subtraction of Col-0. The lower abaxial surface is represented by circles, while the upper adaxial surface by up-pointing triangles. Level of significance of the leaf surface effect within each genotype: ***$P < 0.001$, **$P < 0.01$, and *$P < 0.05$. Level of significance of pairwise ANOVA that compare the susceptibility of each mutant to Col-0: $^{+++}P < 0.001$, $^{++}P < 0.01$, and $^{+}P < 0.05$.
(b) Lesion area and surface differential (abaxial–adaxial lesion area) at 48 HPI (red dots), 72 HPI (green dos), and 96 HPI (blue dots). The high susceptibility double mutant *cyp79b2/b3* is only traced up to 72 HPI, because at 96 HPI, the entire Arabidopsis leaf area is consumed.

To understand how the leaf surfaces and chemical defenses interplayed, we plotted the induced concentration of camalexin, I3M, 4MI3M, and aliphatic glucosinolates across mutants when infected on different surfaces (Figure 4). Interestingly, in the WT controls, there was no statistical support for differential induction depending on the leaf surface that was infected (Figure 4). The mutants however identified differential induction across the leaf surfaces. For example, mutants in the aliphatic glucosinolate TFs (myb28/29) lead to a change in the camalexin response (Figure S6) with a higher response to adaxial than abaxial infection (Figure 4a). Mutants in the

myrosinases (tgg1/2) and the camalexin biosynthetic gene (pad3) led to shifts in indole glucosinolate responses (Figures S8 and S9), again with a higher adaxial than abaxial response (Figure 4b,c). This showed that the differential chemical responses to adaxial/abaxial infection are coordinated across metabolites. The mutants altered the response of indirectly related chemicals, for example aliphatic mutants altered indolic responses and vice versa. Future work will be needed to uncover the specific regulatory mechanisms controlling the differential adaxial and abaxial responses, their dependency on other defenses, and how they vary across leaf surfaces leading to these differences.

B. cinerea genetic diversity impacts the growth on leaf surfaces

Testing how the variation between leaf surfaces influenced host interactions both across and within species using a subset of strains revealed a consistent and major role (e.g. large percentage of variance in lesion area) of genetic variation among Botrytis strains (Figures S1b and S5). This led us to test how genetic variation in the pathogen can influence the measured leaf surface effect. To do this, we infected Arabidopsis Col-0 with a collection of 96 strains of Botrytis and tracked the lesion development on leaf surfaces across time.

To measure the contribution of the pathogen's genetic diversity to lesion development, we modeled the growth of the lesion area on the leaf surfaces (Figure 5a) with a linear model at each time point. The linear models revealed that the diversity of strains accounts for at least 35% of the variance (Figure 5b), which is maximal around 72 HPI. The variance due to abaxial and adaxial leaf surfaces increased from 3% at 48 HPI to 20% of the total variance in lesion area at 96 HPI (Figure 5b). As the genetic diversity in the strain collection is a dominant component controlling the leaf–surface interaction, we investigated the 96 strains for their virulence and surface differential (lesion area on the abaxial–adaxial surface) across the three time points (Figure 5c). The relationship between virulence and surface differential is not consistently linear as various growth patterns are present in the strain collection (Figure 5c). Most strains develop consistently faster on the abaxial surfaces (e.g. strain 1.05.22, Figure 5d), while some stabilize their growth on both surfaces after 72 HPI (e.g., strain 2.04.12, Figure 5d). Other strains have high virulence but a low preference for growth on a surface (e.g., strain 2.04.14, Figure 5d). Finally, a few strains indicate a degree of preference to grow on the adaxial surface (e.g., strain 2.04.04, Figure 5d). These various growth patterns in Botrytis suggest that overall the virulence and the differential surface effect do not rely on identical sets of genes, with genes potentially contributing independently to the two traits.

DISCUSSION

By surveying Botrytis virulence across diverse hosts within the caryophyllales, asterids, and rosids, we showed that the adaxial and abaxial leaf surfaces differentially influence the interaction with Botrytis. However, the effect of the adaxial vs abaxial leaf surface was highly conditional on the host species and pathogen genotype being used. This effect was not linked to differences in classically assumed physical properties such as variation in stomatal density and leaf thickness. This suggests that there are other unmeasured physical, mechanistic, or microbiome (Berens et al., 2019; Liu et al., 2020; Ritpitakphong et al., 2016; Schäfer et al., 2023) components that are critical to the adaxial and abaxial effects on Botrytis interactions and that they may differ from host to host. Thus, mechanistic insights might not be fully translatable between host species.

Testing 96 strains of *B. cinerea* further complicated the modeling of the mechanistic insights. This showed that the strains within the pathogen species have a wide range of different patterns of interaction with the leaf surfaces (Figure 5). This ranged from strains that better attacked the adaxial to those with better invasiveness on the abaxial to those with no significant difference. Whether that complex interaction is a sum of independent mechanisms adding together in the host and pathogen or whether those are representative of molecular mechanisms with different interactions based on leaf surface remains to be determined. Given the wide range of hosts (Singh et al., 2023) and organs attacked by Botrytis and the polygenic nature of its virulence (Caseys et al., 2021; Soltis et al., 2019), it is challenging to know whether those growth patterns might result from genes' presence/absence variation (Simon et al., 2022), single nucleotide polymorphisms (Caseys et al., 2021) or plasticity in the regulation of virulence pathways. Furthermore, how various strains detect the hosts' extracellular signals and mount diverse responses/strategies at different times post-inoculation remains largely unknown. Botrytis has over a thousand surface-associated proteins that might contribute to detecting the host (Escobar-Niño et al., 2021), with signal transduction best described through the interplay of cAMP, MAP-kinase, histidine-kinase, and calcium-dependent signaling pathways (Liñeiro et al., 2016). Even in the absence of precise mechanisms, it remains striking how conditional the host–Botrytis interaction is to genetic variation in both the host and pathogen when querying the differences in leaf surfaces.

Using Arabidopsis mutants that altered differently the SA and JA defense signaling pathways began to illuminate some of the mechanisms involved. Once the pathogen is detected on a leaf surface and immunity is triggered (Kushalappa et al., 2016; Zipfel, 2008), defense response signals

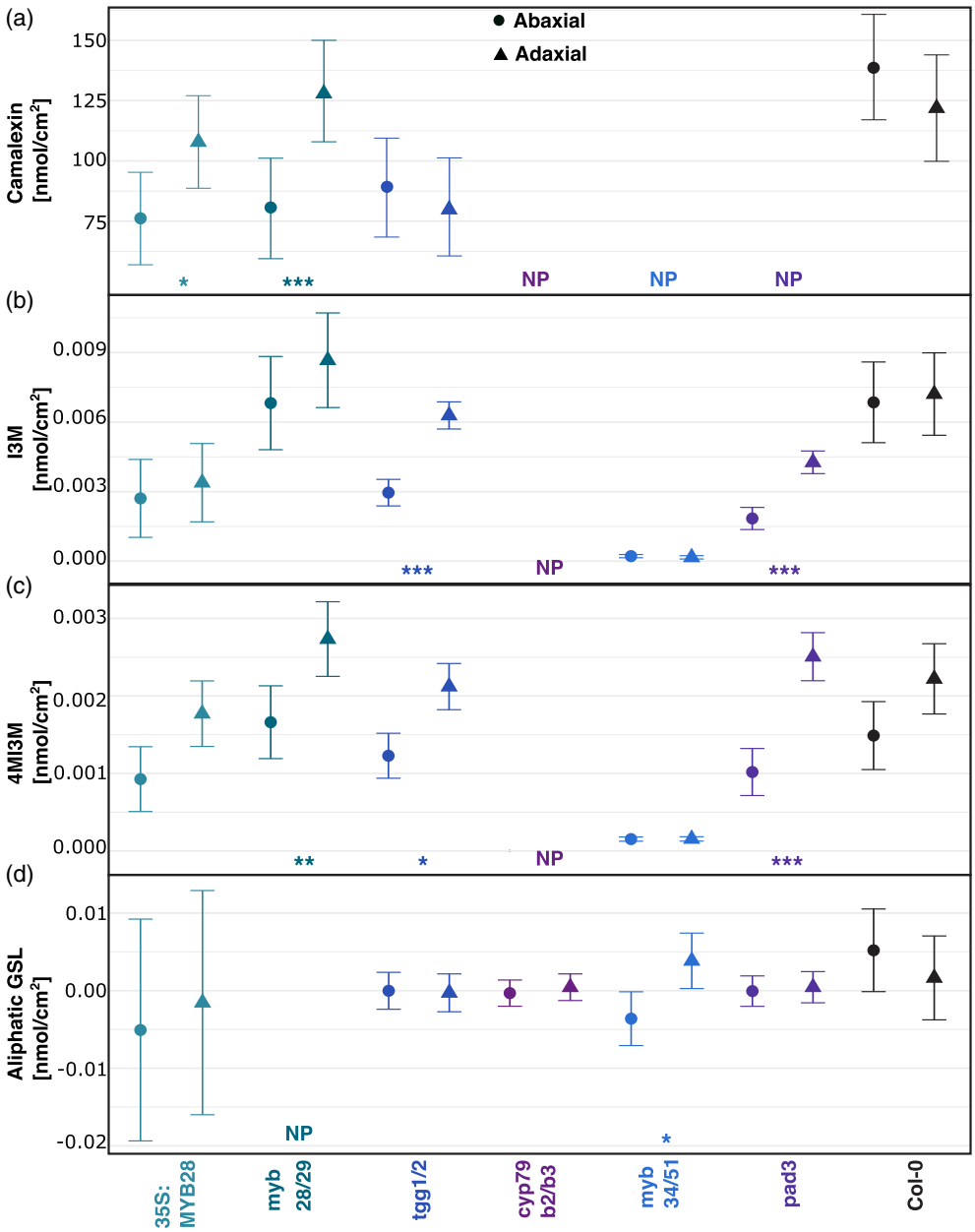

Figure 4. Infections with *B. cinerea* on leaf surfaces of *A. thaliana* mutants differentially induced phytochemical defenses. Indolic and aliphatic glucosinolates responses are calculated by subtraction of the mean of concentration of the uninfected leaves to the infected leaves. Camalexin is only present in infected leaves and did not require normalization. The lower abaxial surface is represented by circles, while the upper adaxial surface by up-pointing triangles.
(a) Mean and standard error bars (n = 10 strains*4 replicates) of the camalexin in nmol/cm^2.
(b) Mean and standard error bars (n = 10 strains*2 replicates) of the indol-3-yl-methyl glucosinolate (I3M) in nmol/cm^2.
(c) Mean and standard error bars (n = 10 strains*2 replicates) of the 4-methoxy-indole-3-yl-methyl glucosinolate (4MI3M) in nmol/cm^2.
(d) Mean and standard error bars (n = 10 strains*2 replicates) of total aliphatic glucosinolates in nmol/cm^2. (a–d) Level of significance: ***$P < 0.001$, **$P < 0.01$, and *$P < 0.05$. NP stands for "not present." The mutants *cyp79b2/b3*, *myb34/51* (Schlaeppi et al., 2010), and *pad3* (Zhou et al., 1998) do not produce camalexin. The mutant *cyp79b2/b3* does not produce indolic glucosinolates, while *myb34/51* does not fully stop their synthesis, probably due to accessory role of MYB122 (Frerigmann & Gigolashvili, 2014). The mutant *myb28/29* does not produce aliphatic glucosinolates (Sonderby et al., 2010).

are integrated into complex networks, with SA and JA signaling in competitive intercommunications. This complex signal integration is beneficial to canalize the range of virulence both within and between pathogens species by fine-tuning the immune response (Caarls et al., 2015; Hou & Tsuda, 2022; Zhang et al., 2017). This showed that Arabidopsis SA signaling mutants (*pad4*, *npr1*) (Ferrari et al., 2003) have strong surface effects while do not

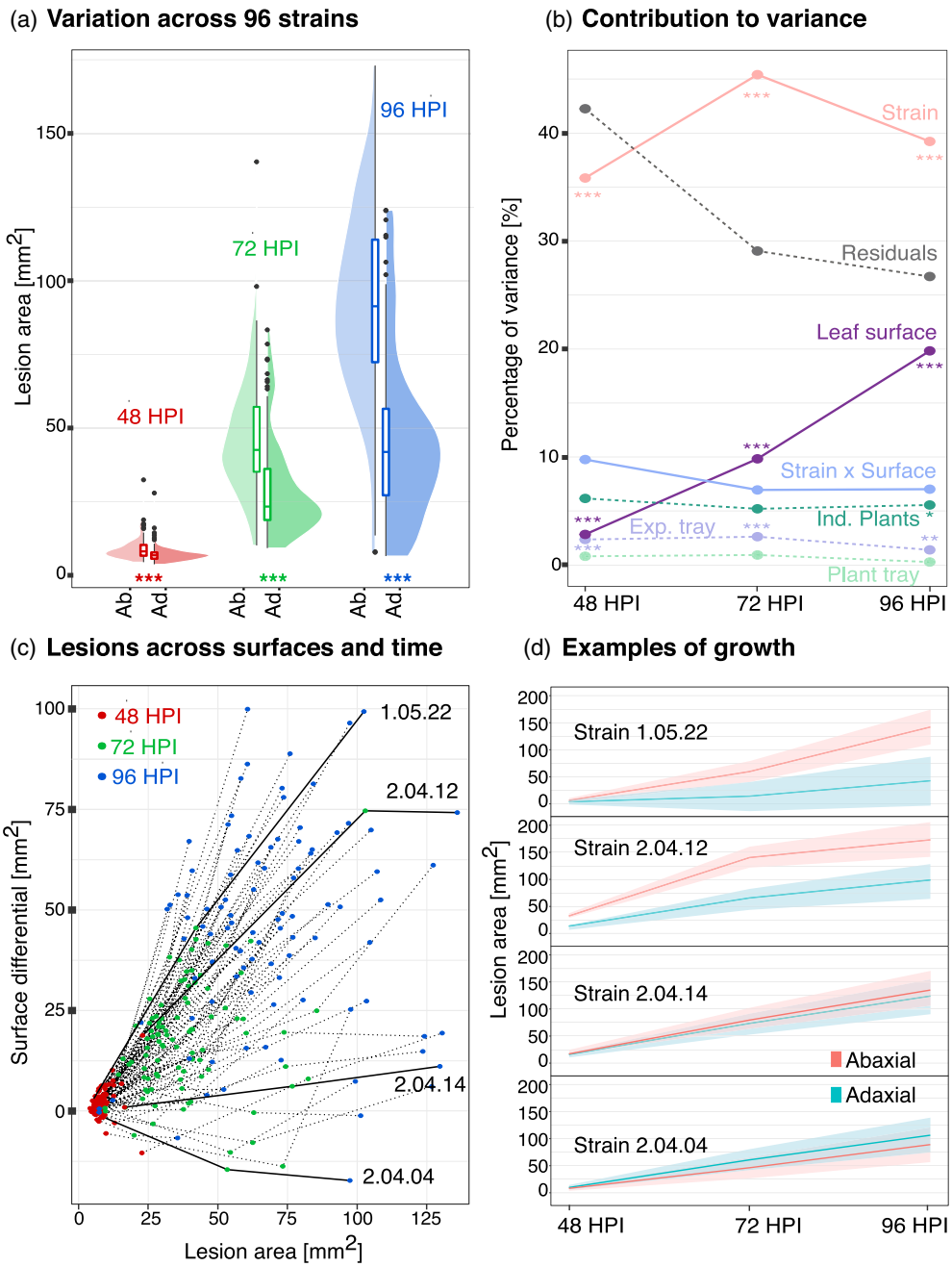

Figure 5. *B. cinerea* genetic diversity across of 96 strains ($n = 4$) impacts the growth on *A. thaliana* (Col-0) abaxial and adaxial surfaces. Significance: ***$P < 0.001$; **$P < 0.01$; and *$P < 0.05$.

(a) Distribution of lesion area across Botrytis 96 strains at 48 HPI (in red), 72 HPI (in green), and 96 HPI (in blue).

(b) Percentages of variance calculated by linear modeling of the lesion area at 48, 72, and 96 HPI. Plain lines represent the biological factors, while dashed lines represent technical factors and residuals.

(c) Lesion development of 96 Botrytis strains represented by the lesion area across both surfaces (*x*-axis) and the difference in lesion area (abaxial–adaxial) across leaf surfaces (*y*-axis).

(d) Mean and 95% confidence interval of the lesion area of the four strains highlighted in panel c.

increase the overall plant susceptibility (Figure 3b), whereas JA signaling mutants (*coi1*, *anac055*) (Rowe et al., 2010) impacted the plant susceptibility without influencing the adaxial/abaxial difference (Figure 3b). This suggests that JA may influence Botrytis defense independently of the surface, while SA may have differential effects across the surfaces. Such spatiotemporal developmental patterns were also recently described in Barley with

variation in response to JA and gibberellins across the leaf blade infected by *Blumeria hordei* (Krasauskas et al., 2023). In Arabidopsis leaves infected with powdery mildew, higher resistance of the abaxial surface was explained by defenses associated with both SA pathway and glucosinolates (Wu et al., 2023). Thus, the core defense pathways may differentially contribute to how Arabidopsis defends against adaxial or abaxial Botrytis invasion.

In Arabidopsis–Botrytis interactions, major SA/JA pathway outputs that control the interaction are the production of camalexin and glucosinolate defense metabolites regulated by MYBs. From our experiment, indolic-associated MYB34 and MYB51 increased the surface effect, aliphatic-associated MYB28 diminished the surface effect, and the other aliphatic-associated MYB had a time-dependent effect. These MYBs are known to have altered expression in Arabidopsis mutants with altered ad-abaxial development (Malitsky et al., 2008). These MYBs also showed abaxial/adaxial patterning in the shoot apical meristem atlas at an early stage of bifacial leaf development (Tian et al., 2019), with MYB51 preferentially expressed on the abaxial, while MYB28, MYB29, and MYB34 are preferentially expressed on the adaxial domain. Although these MYBs follow the developmental pattern, whether de novo synthesis at the site of the attack generated differential production of chemical defenses (Figure 4) or whether those patterns also resulted from the strategic movement of defenses within the leaf remains largely unknown (Burow & Halkier, 2017). Though differential induction of indolic glucosinolates and camalexin might contribute to the surface effect, these defense compounds are restricted to the Brassicaceae. Given that the surface effect is spread across the eudicots, other phytoalexins might have similar differential induction in other eudicot species. This is similar to the observation that lineage-specific phytoalexins and specialized metabolites are often controlled by the conserved JA/SA signaling pathways (Lacchini & Goossens, 2020; Rieseberg et al., 2023).

While the complexity of how abaxial and adaxial surfaces regulate genes and metabolites is only starting to be addressed, how those react to a pathogen infection remains largely unaddressed. Single-cell sequencing of Arabidopsis infected by the biotroph fungal pathogen *Colletotrichum higginsianum* revealed the spatially dynamic and cell-type specific plant response (Tang et al., 2023). Although the fungal infections were inoculated only on the adaxial surface, they especially show the crucial role of intracellular immune receptors (NLRs) across cell types and cell-specific induction of indolic glucosinolates. Future experiments will need to confirm the differential expression of immune receptors and other defense components not only across cell types but also along the abaxial–adaxial axis.

To conclude, this study provides a snapshot into how conditional plant–pathogen interactions are. They depend on small-scale developmental pattern such as leaf surfaces to population-level patterns such as the diversity in both the host and pathogen. This illustrates a potential ascertainment bias in foliar infection studies: Most infection assays to validate genes and determine mechanisms are necessarily done on a single surface, typically adaxial, to make the experiments feasible. However, the pathogens or plant mutants/genotypes may show differential behavior if infected on the abaxial surface and this will vary across hosts and pathogens complicating the ability to make broad mechanistic conclusions. To determine precisely the signaling cascade and gene networks responsible for the differential interactions on the two leaf surfaces will require both host and pathogen transcriptomes to be analyzed in detail with single-cell experiments in three dimensions across the time of the infection using multiple hosts and pathogen genotypes. Conducting such an experiment is currently limited by available technology, such as the absence of a cell atlas for Botrytis. As new technologies that will preserve the special context of tissues lift these restrictions, it will become possible to develop deeper mechanistic insights and understand how they may or may not translate across host species and pathogen genotypes (Nolan & Shahan, 2023).

MATERIALS AND METHODS

Genotype selection and plant growth

Sixteen crop species (Figure 1a; Table S1) were selected within the Rosids, Asterids, and caryophyllales. For the Rosids, *Brassica oleacera* (kale), *Raphanus sativus* (radish), *Cucumis sativus* (cucumber), *Vigna unguicula* (cowpea) and *Phaseolus vulgaris* (common bean) were selected. For Asterids, *Petroselinum crispum* (parsley), *Cichorium intybus* (chicory), *Lactuca sativa* (lettuce), *Ocimum basilicum* (basil), *Mentha spicata* (mint), *Solanum melongena* (eggplant), *Solanum lycopersicum* (tomato), *and Capsicum annuum* (pepper) were selected. For caryophyllales, *Beta vulgaris* (swiss chard) and *Spinacia oleracea* (spinach) were selected. Plants were grown from seeds (Table S1) in a single growth chamber at 20°C, 60% humidity with 16 hours of daylight at 100–120 μE light intensity. All plants were grown in Sunshine Mix#1 (Sun Gro Horticulture, Agawam, MA) horticulture soil and watered with nutrient solution (0.5% N-P-K fertilizer in a 2-1-2 ratio; Grow More 4-18-38).

Twenty *Arabidopsis thaliana* genotypes and mutants were used in this study (Figure 1b; Table S2). In addition to Col-0, the background accessions for all mutants, the Ler accession was used to control for whole genome-wide variation. For defense signaling, two SA and three JA mutants were selected (Figure 1b; Table S2) (Bu et al., 2008; Cao et al., 1997; Ellis & Turner, 2002; Miao et al., 1994; Zhou et al., 1998). The mutant coi1-16 was backcrossed to remove pen2 and gl1 mutations. For chemical defenses, mutants for both the methionine-derived (aliphatic glucosinolates) (Barth & Jander, 2006; Sonderby et al., 2010; Sønderby et al., 2007; Zhou et al., 1998) and tryptophan-derived (indolic glucosinolates, camalexin, Indole-cyanogenic glycosides)

(Frerigmann & Gigolashvili, 2014; Mikkelsen et al., 2003; Rajniak et al., 2015; Zhou et al., 1998) pathways were selected (Figure 1b; Table S2). All Arabidopsis seeds were cold-stratified in deionized water for three days at 4°C and sown on the soil. After sowing, Arabidopsis plants grew at 20°C with 10 h photoperiod at 100–120 μE light intensity. All Arabidopsis plants were grown for 8 weeks in cell flats containing Sunshine Mix#1 (Sun Gro Horticulture, Agawam, MA) horticulture soil. They were watered twice weekly with deionized water for the first 2 weeks and then with nutrient solution (0.5% N-P-K fertilizer in a 2-1-2 ratio; Grow More 4-18-38).

Botrytis growth and collection

A collection of 96 *B. cinerea* strains (Table S3) was used in this study. These strains were primarily isolated on grapevine in California, and no signs of host specialization were detected (Soltis et al., 2019). All those strains were previously characterized across eight eudicots (Caseys et al., 2021) and on Arabidopsis (Zhang et al., 2017). Their virulence was calculated as the average z-scaled value of lesion formation across hosts, while their host specificity was estimated based on the coefficient of variation across hosts (Caseys et al., 2021). Camalexin sensitivity was estimated as the differential in lesion formation of the strains on Arabidopsis genotypes that can (Col-0) or cannot make camalexin (pad3) (Zhang et al., 2017). The strains were maintained by spore collections for long-term preservation as conidial suspension in 60% glycerol at −80°C. For each experiment, the strains were grown from spores on peach slices at 21°C for 2 weeks.

Detached leaf assay

The virulence of the strains on each species was measured using detached leaf assays (Denby et al., 2004). The experiments included four to six replicates (see each experiment section) for each Botrytis strain × leaf surface × host genotype in a randomized complete block design. In brief, mature (non-juvenile) fully developed leaves were cut from the eight-week-old adult plants in the vegetative phase before bolting initiation. The leaves, either on the abaxial or on the adaxial surface, were deposited on 1 cm of 1% phytoagar to provide water to maintain the leaf for the duration of the experiment. Botrytis spores were collected in sterile water, counted with a hemacytometer, and sequentially diluted with 50% grape juice to 10 spores/μl. Drops of 4 μl (40 spores of Botrytis) were used to inoculate the leaves. All inoculations were synchronized to the late afternoon to minimize the effect of the circadian rhythm. The inoculated leaves were maintained under humidity domes under constant light at room temperature. The experimental trays were pictured every 24 h. The lesion area on each leaf was measured from the images with a custom-R script (Fordyce et al., 2018). Images were transformed into hue/saturation/value (HSV) color space. Masks marking the leaves and lesions were created by the script using color thresholds and confirmed manually. The lesions were measured by counting the number of pixels of the original pictures within the area covered by the lesion mask. The numbers of pixels were converted into centimeters using a reference scale within each image.

Statistical analyses

All data handling and statistical analyses were conducted in R. For each experiment, the contribution of the host resistance, leaf surfaces, pathogen virulence, and their interactions was estimated by linear modeling of the lesion area, while correcting for the micro-environmental effect. Micro-environmental effects are due to the randomized complete block design of the detached leaf assays within experimental trays and are considered as a random factor. The ANOVA sums of squares were converted into a percentage of total variance to ease the comparison across plants and experiments. Given the experimental design allowing for control for the micro-environment variation, random effect adjusted means (least-square means) (Lenth, 2016; Martín-Cacheda et al., 2024; Naets et al., 2020; Sbeiti et al., 2023) rather than arithmetic means were calculated. The least-square means adjusted for experimental effects and standard errors were calculated with the emmeans package using the Satterthwaite approximation (Lenth, 2016). Specific models are further described within each experimental design section.

Eudicot experiment

Using the detached leaf assay described above, 10 Botrytis strains (Apple517, B05.10, Davis Navel, 2.04.12, Kern B1, Katie Tomato, Pepper, Rose, Triple 3, UKrazz, Table S3) were inoculated on either leaf surface of each host species (Table S1) in a 6-fold replication resulting in 1832 observations. The 10 Botrytis strains sample the range of virulence and host specificity observed within the full collection of 96 strains (Caseys et al., 2021). The observations were cleaned for failed lesions (technical failures without Botrytis growth) following Caseys et al., 2021, removing 127 observations. To characterize the contribution of Botrytis strains, the leaf surfaces, and their interaction, the lesion area was modeled for each species with a linear model: Lesion area ~ Strain × Surface. To test the developmental effect of the leaf surface independently of the strain effect, the least-square mean and standard error were modeled within each species with a linear mixed model: Centered_Lesion ~ Surface +1|Strain +1|Tray, where the effect of the Botrytis strains and experimental tray were considered as random effects. Given the different resistance profiles of the 16 eudicot species (Figure S1a), the lesion areas on each surface were centered by subtraction of the mean lesion area of each species. The same method was applied to the stomata density.

To observe the leaf surface and count stomata, the adaxial/abaxial leaf surfaces of the 16 plant species were molded by applying gel cyanoacrylate super glue (the original super glue corporation) on microscope slides and then embedding the leaf on the glue (Castilloa & Ferrarotto, 1998). After drying, the leaf profiles were cleaned in 0.1% anionic detergent solution (Alconox). A Leica CME microscope was used to observe and picture slides.

Arabidopsis experiment

Using the detached leaf assay described above, ten *B. cinerea* strains (1.03.04, 2.04.17, Apple517, KernB1, Katie Tomato, Pepper, Rasp, Rose, Triple 3, UKrazz, Table S3) were inoculated on either leaf surface of each host genotype (Table S2) in a 4-fold replication resulting in 1600 observations, from which 107 were considered as technical failures and removed. The 10 Botrytis strains sample the range of virulence (Caseys et al., 2021) and sensitivity to camalexin (Zhang et al., 2017) observed within the full collection of 96 strains (Table S3). The lesion areas were centered by subtracting the least-square mean of the lesion area of Col-0, the background accession. This centering allows directly observing the effect of the gene overexpression or knockout by removing the effect of the genetic background. The surface differential was calculated by subtraction of the least-square mean of the lesion area of the adaxial surface to the least-square mean of the lesion area of the abaxial surface. Therefore, a negative surface differential indicates preferential growth on the adaxial surface, while a positive surface differential indicates preferential growth

on the abaxial surface. Because we aimed to test the developmental effect of the leaf surface independently of the effect of the strain, the least-square mean and standard error were modeled within each genotype with a linear mixed model: Centered_Lesion ~ Surface +1|Strain +1|Tray, where the effect of the Botrytis strains and experimental tray were considered as random effects.

To detect the effect of Botrytis on *A. thaliana* chemical defenses, Col-0, *myb28/29* (Sonderby et al., 2010), the overexpression *35S:MYB28* (Sønderby et al., 2007), *tgg1/2* (Barth & Jander, 2006), *myb34/51* (Frerigmann & Gigolashvili, 2014), *pad3* (Zhou et al., 1998), and *cyp79b2/b3* (Mikkelsen et al., 2003) genotypes were inoculated on either the abaxial or adaxial surface with 40 spores. These mutants were selected to model a range of chemotypes, with high or low methionine/tryptophan-derived chemicals and the absence of myrosinase. For each genotype and each surface, infected and uninfected leaves at 72 h post-inoculation (HPI) were transferred into tubes containing 400 μl of 90% methanol. The leaves were ground in the methanol for 3 min using metal beads and a tissue disruptor. After centrifugation, 150 μl of the supernatant was transferred on filter plates containing Sephadex DEAE A-25. The first flow through from centrifugation was analyzed for camalexin. Glucosinolates were washed with 90% methanol and water, before sulfatase incubation overnight (Kliebenstein et al., 2001). An injection of 50 μL of Desulfoglucosinolate solution was run on an Agilent LiChroCART 250–4 RP18e 5 μm column using an Agilent 1100 series HPLC system. Separation was achieved using the following solvent gradient with 1.5 to 5% acetonitrile in 6 min, 7% at 8 min, 25% at 15 min, 92% at 17 min and reconditioning of the column in 25 min. Glucosinolates were detected with a diode array detector at 229 nm. For camalexin, 20 μl was injected and separation was achieved with a gradient of aqueous acetonitrile from 31% to 69% acetonitrile in 5 min, 50 sec to 99%, and reconditioning in 8 min. Camalexin was detected with a fluorescence detector at emission 318 nm/excitation 385 nm. To normalize the concentrations of glucosinolate (GSL) and camalexin across leaves, all detached leaves at 72 HPI were pictures before extraction. The square centimeter of leaf area was then used for normalization. Aliphatic glucosinolates are the sum of 3-Methylsulfinylpropyl *GSL* (3MSO), 4-Methylsulfinylbutyl GSL (4MSO), 4-Methylthio GSL (4MT), 5-Methylsulfinylpentyl GSL (5MSO), 6-Methylsulfinylhexyl GSL (6MSO), 7-Methylsulfinylheptyl GSL (7MSO), and 8-Methylsulfinyloctyl GSL (8MSO). Indolic glucosinolates are the sum of indole-3-yl-methyl GSL (I3M), 4-methoxy-indole-3-yl-methyl GSL (4MI3M), and 4-hydroxy-indole-3-yl-methyl GSL (4OHI3M). To estimate the percentage of variance in lesion area, linear modeling across six mutants and Col-0 was performed based chemical content with the formula: Lesion ~ Strain × Surface × Camalexin + aliphatic + indolic. Linear regressions between lesion area and camalexin, I3M, 4MI3M, or aliphatic glucosinolates were also performed for each genotype in which the targeted compound was detected.

For further condensing the information into a single figure, the data were mean-centered by the subtraction of the mean concentration of the mock (not infected leaves) in each genotype for each compound. This mean centering allowed us to directly plot the concentration induced by the pathogen on each leaf surface. The data for camalexin were not mean-centered, given that camalexin is not constitutively synthesized in Arabidopsis and uninfected leaves do not produce camalexin. For each compound, a linear mixed model was used to model the least-square means and standard error: concentration ~ Surface +1|Strain +1|Tray, where the effect of the Botrytis strains and experimental tray were considered as a random effect.

To detect the mode of infection of Botrytis on *A. thaliana* leaf surfaces, Col-0, *myb28/29* (Sonderby et al., 2010), the overexpression *35S:MYB28* (Sønderby et al., 2007), *tgg1/2* (Barth & Jander, 2006), *myb34/51* (Frerigmann & Gigolashvili, 2014), *pad3* (Zhou et al., 1998), and *cyp79b2/b3* (Mikkelsen et al., 2003) genotypes were sprayed on either abaxial or adaxial surface with water containing 10 spores/μl. After 24, 36, 42, 48, and 72 h post-inoculation, leaves were cleared with acetic acid–ethanol 1:3 v/v solution for 3 h. They were cleared with acetic acid–ethanol–glycerol 1:5:1 v/v/v solution for another 3 h. The leaves were stained with lactic acid–glycerol–water 1:1:1 v/v/v containing 0.05% trypan blue. Leaves were mounted on microscope slides after rinsing in 60% glycerol.

Botrytis diversity experiment

Using the detached leaf assay described above, we infected Col-0 detached leaves with a 96 strains from Botrytis (Caseys et al., 2021) in a 4-fold replication resulting in 792 observations. The 96 strains include the various strains tested in the Eudicot and Arabidopsis experiments mentioned above (Table S3). The lesion area was modeled with a linear model Lesion_Area ~ Strain × Surface + Experiment_Tray + Individual_Plant. Strain and surface are biological factors, while experimental tray and the individual plant from which the leaves were collected are technical factors.

AUTHOR CONTRIBUTIONS

Conceptualization: CC and DJK; Supervision: DJK; Data analysis: CC; Funding acquisition: DJK; Investigation: CC, AJM, JV, MA, AH, DK, SK, MM, TP, and MW; and Writing: CC, AJM, and DJK.

ACKNOWLEDGMENTS

This work was initiated by a curiosity-driven question of an undergraduate student asking why we inoculated only the adaxial surface. Undergraduate students also largely conducted the experiments and observations. This work was supported by the NSF award IOS 2020754 and USDA award 2019-05709 to DJK.

CONFLICT OF INTEREST

None declared.

DATA AVAILABILITY STATEMENT

Correspondence and requests for materials should be addressed to kliebenstein@ucdavis.edu. The datasets and R codes are available on Dryad. https://doi.org/10.5061/dryad.r4xgxd2p6

SUPPORTING INFORMATION

Additional Supporting Information may be found in the online version of this article.

Figure S1. The susceptibility of leaf surfaces to *B.cinerea* vary across the eudicots and the variation is largely explained by the strains' diversity.

Figure S2. Leaf thickness and stomata density don't explain the differential in lesion area on the ab/adaxial surfaces across 16 eudicot hosts.

Figure S3. Microscopy of *B. cinerea on Arabidopsis leaf surfaces across a time course did not result in observation of entry through stomata but developmentally diverse infection cushion structures.*

Figure S4. Concentration [nmol/cm^2] of glucosinolates in leaves with and without (n = 4) Botrytis infection (n = 10 strains * 2 replicates) on the abaxial (green) or adaxial (brown) surface.

Figure S5. Parsing the effects of Botrytis diversity, leaf surfaces and chemical defenses.

Figure S6. Camalexin acted as a phytoalexin and negatively impacted Botrytis growth.

Figure S7. Aliphatic glucosinolates negatively impact the lesion area in Col-0, myb34/51 and cyp79b2/b3.

Figure S8. I3M negatively impact the lesion area in Col-0, tgg1/2 and pad3.

Figure S9. 4MI3M had no strong effects on the lesion area.

Table S1. Information on the 16 eudicot species used to test how the leaf surfaces influence host-Botrytis interactions across species. In addition to the information on the seeds' origin, the average leaf thickness, stomata density and lesion area on each leaf surface are provided.

Table S2. Information on the 20 *A. thaliana* genotypes used to test how leaf surfaces change the interaction with Botrytis within a species. Mutants are deficient in SA and JA defense signaling, aliphatic and indolic glucosinolates, putative cyanogenic glycosides, and camalexin biosynthesis.

Table S3. Information on the 96 *B. cinerea* strains used in this study. For each strain the geographical origin, the host it was isolated from (not equal to host specialization or pathovars) are provided. Values for general virulence and host specificity (Caseys et al., 2021) and camalexin sensitivity (Zhang et al., 2017) were used to subset the 10 strains associated to the Eudicot and Arabidopsis experiments. Which strain was used in which experiment (Eudicots, Arabidopsis, and/or Botrytis96) is also provided.

REFERENCES

Aragón, W., **Reina-Pinto, J.J.** & **Serrano, M.** (2017) The intimate talk between plants and microorganisms at the leaf surface. *Journal of Experimental Botany*, **68**(19), 5339–5350.

Atwell, S., **Corwin, J.A.**, **Soltis, N.**, **Zhang, W.**, **Daniel Copeland, J.F.**, **Eshbaugh, R.** ***et al.*** (2018) Resequencing and association mapping of the generalist pathogen *Botrytis cinerea*. *bioRxiv*, **7**(8), e1002230.

Ballhorn, D.J., **Kautz, S.**, **Jensen, M.**, **Schmitt, I.**, **Heil, M.** & **Hegeman, A.D.** (2011) Genetic and environmental interactions determine plant defences against herbivores. *Journal of Ecology*, **99**(1), 313–326.

Barth, C. & **Jander, G.** (2006) Arabidopsis myrosinases TGG1 and TGG2 have redundant function in glucosinolate breakdown and insect defense. *The Plant Journal*, **46**(4), 549–562.

Berens, M.L., **Berry, H.M.**, **Mine, A.**, **Argueso, C.T.** & **Tsuda, K.** (2017) Evolution of hormone signaling networks in plant defense. *Annual Review of Phytopathology*, **55**, 401–425.

Berens, M.L., **Wolinska, K.W.**, **Spaepen, S.**, **Ziegler, J.**, **Nobori, T.**, **Nair, A.** ***et al.*** (2019) Balancing trade-offs between biotic and abiotic stress responses through leaf age-dependent variation in stress hormone cross-talk. *Proceedings of the National Academy of Sciences*, **116**(6), 2364–2373.

Bi, K., **Liang, Y.**, **Mengiste, T.** & **Sharon, A.** (2022) Killing softly: a roadmap of *Botrytis cinerea* pathogenicity. *Trends in Plant Science*, **28**(2), 211–222.

Bu, Q., **Jiang, H.**, **Li, C.-B.**, **Zhai, Q.**, **Zhang, J.**, **Wu, X.** ***et al.*** (2008) Role of the Arabidopsis thaliana NAC transcription factors ANAC019 and ANAC055 in regulating jasmonic acid-signaled defense responses. *Cell Research*, **18**(7), 756–767.

Burow, M. & **Halkier, B.A.** (2017) How does a plant orchestrate defense in time and space? Using glucosinolates in Arabidopsis as case study. *Current Opinion in Plant Biology*, **38**, 142–147.

Buxdorf, K., **Yaffe, H.**, **Barda, O.** & **Levy, M.** (2013) The effects of Glucosinolates and their breakdown products on necrotrophic fungi. *PLoS One*, **8**(8), e70771.

Caarls, L., **Pieterse, C.M.J.** & **Van Wees, S.C.M.** (2015) How salicylic acid takes transcriptional control over jasmonic acid signaling. *Frontiers. Plant Science*, **6**, 170.

Caires, N.P., **Rodrigues, F.A.** & **Furtado, G.Q.** (2014) Infection process of b*otrytis cinerea* on eucalypt leaves. *Journal of Phytopathology*, **163**(7–8), 604–611.

Calo, L., **García, I.**, **Gotor, C.** & **Romero, L.C.** (2006) Leaf hairs influence phytopathogenic fungus infection and confer an increased resistance when expressing a Trichoderma α-1, 3-glucanase. *Journal of Experimental Botany*, **57**(14), 3911–3920.

Cao, H., **Glazebrook, J.**, **Clarke, J.D.**, **Volko, S.** & **Dong, X.** (1997) The Arabidopsis NPR1 gene that controls systemic acquired resistance encodes a novel protein containing ankyrin repeats. *Cell*, **88**(1), 57–63.

Caseys, C., **Shi, G.**, **Soltis, N.**, **Gwinner, R.**, **Corwin, J.A.**, **Atwell, S.** ***et al.*** (2021) Quantitative interactions: the disease outcome of *Botrytis cinerea* across the plant kingdom. *G3*, **11**(8), jkab175.

Castilloa, J.J. & **Ferrarotto, M.** (1998) Evaluation of cyanoacrylate glues for making attached living-leaves epidermis replicas and its scanning electron microscopy observations (evaluación de pegamentos de cianoacrilato para hacer réplicas epidérmicas en hojas vivas adheridas y su observación al MEB). *Scanning*, **20**(8), 557–563.

Choquer, M., **Rascle, C.**, **Gonçalves, I.R.**, **de Vallée, A.**, **Ribot, C.**, **Loisel, E.** ***et al.*** (2021) The infection cushion of *Botrytis cinerea*: a fungal 'weapon' of plant-biomass destruction. *Environmental Microbiology*, **23**(4), 2293–2314.

Chung, K.-M., **Igari, K.**, **Uchida, N.** & **Tasaka, M.** (2008) New perspectives on plant defense responses through modulation of developmental pathways. *Molecules and Cells*, **26**(2), 107–112.

da Silva, R.-F.H., **Coca Ruíz, V.**, **Suárez, I.**, **Moraga, J.**, **Aleu, J.** & **Collado, I.G.** (2023) From genes to molecules, secondary metabolism in *Botrytis cinerea*: new insights into anamorphic and Teleomorphic stages. *Plants*, **12**(3), 553.

Denby, K.J., **Kumar, P.** & **Kliebenstein, D.J.** (2004) Identification of *Botrytis cinerea* susceptibility loci in *Arabidopsis thaliana*. *The Plant Journal*, **38**(3), 473–486.

Ellis, C. & **Turner, J.G.** (2002) A conditionally fertile coi1 allele indicates cross-talk between plant hormone signalling pathways in Arabidopsis thaliana seeds and young seedlings. *Planta*, **215**(4), 549–556.

Endara, M.-J., **Forrister, D.L.** & **Coley, P.D.** (2023) The evolutionary ecology of plant chemical defenses: from molecules to communities. *Annual Review of Ecology, Evolution, and Systematics*, **54**, 107–127.

Escobar-Niño, A., **Carrasco-Reinado, R.**, **Morano, I.M.**, **Cantoral, J.M.** & **Fernandez-Acero, F.J.** (2021) Unravelling the initial triggers of *Botrytis cinerea* infection: first description of its Surfactome. *Journal of Fungi*, **7**(12), 1021.

Feechan, A., **Turnbull, D.**, **Stevens, L.J.**, **Engelhardt, S.**, **Birch, P.R.J.**, **Hein, I.** ***et al.*** (2015) The Hypersensitive Response in PAMP- and Effector-Triggered Immune Responses. In: Gunawardena, A.N. & McCabe, P.F. (Eds.) *Plant Programmed Cell Death*. Cham: Springer International Publishing, pp. 235–268.

Fernández, V., **Bahamonde, H.A.**, **Javier Peguero-Pina, J.**, **Gil-Pelegrín, E.**, **Sancho-Knapik, D.**, **Gil, L.** ***et al.*** (2017) Physico-chemical properties of plant cuticles and their functional and ecological significance. *Journal of Experimental Botany*, **68**(19), 5293–5306.

Ferrari, S., **Plotnikova, J.M.**, **De Lorenzo, G.** & **Ausubel, F.M.** (2003) Arabidopsis local resistance to *Botrytis cinerea* involves salicylic acid and camalexin and requires EDS4 and PAD2, but not SID2, EDS5 or PAD4. *The Plant Journal*, **35**(2), 193–205.

Ferreira, R.B., **Monteiro, S.**, **Freitas, R.**, **Santos, C.N.**, **Chen, Z.**, **Batista, L.M.** ***et al.*** (2006) Fungal pathogens: the Battle for plant infection. *Critical Reviews in Plant Sciences*, **25**(6), 505–524.

Fillinger, S. & **Elad, Y.** (2016) *Botrytis-the fungus, the pathogen and its management in agricultural systems*. Cham, Switzerland: Springer International Publishing.

Fordyce, R.F., **Soltis, N.E.**, **Caseys, C.**, **Gwinner, R.**, **Corwin, J.A.**, **Atwell, S.** ***et al.*** (2018) Digital imaging combined with genome-wide association mapping links loci to plant-pathogen interaction traits. *Plant Physiology*, **178**(3), 1406–1422.

Forlani, S., **Masiero, S.** & **Mizzotti, C.** (2019) Fruit ripening: the role of hormones, cell wall modifications, and their relationship with pathogens. *Journal of Experimental Botany*, **70**(11), 2993–3006.

Foster, A.S. (1936) Leaf differentiation in angiosperms. *Botanical Review*, **2**(7), 349–372.

Frerigmann, H. & **Gigolashvili, T.** (2014) MYB34, MYB51, and MYB122 distinctly regulate indolic glucosinolate biosynthesis in Arabidopsis thaliana. *Molecular Plant*, **7**(5), 814–828.

Govrin, E.M. & **Levine, A.** (2000) The hypersensitive response facilitates plant infection by the necrotrophic pathogen *Botrytis cinerea*. *Current Biology*, **10**(13), 751–757.

Hashim, M., **Roberts, J.A.**, **Rossall, S.** & **Dickinson, M.J.** (1997) Leaflet abscission and phytoalexin production during the response of two faba bean breeding lines to botrytis infection. *Plant Pathology*, **46**(6), 989–996.

Hou, S. & **Tsuda, K.** (2022) Salicylic acid and jasmonic acid crosstalk in plant immunity. *Essays in Biochemistry*, **66**(5), 647–656.

Hsieh, T.F., **Huang, J.W.** & **Hsiang, T.** (2001) Light and scanning electron microscopy studies on the infection of oriental lily leaves by Botrytis elliptica. *European Journal of Plant Pathology*, **107**(6), 571–581.

Hu, L. & **Yang, L.** (2019) Time to fight: molecular mechanisms of age-related resistance. *Phytopathology*, **109**(9), 1500–1508.

Jeblick, T., **Leisen, T.**, **Steidele, C.E.**, **Albert, I.**, **Müller, J.**, **Kaiser, S.** ***et al.*** (2023) Botrytis hypersensitive response inducing protein 1 triggers non-canonical PTI to induce plant cell death. *Plant Physiology*, **191**(1), 125–141.

Kazan, K. & **Manners, J.M.** (2009) Linking development to defense: auxin in plant–pathogen interactions. *Trends in Plant Science*, **14**(7), 373–382.

Kidner, C.A. & **Timmermans, M.C.P.** (2010) Signaling sides adaxial-abaxial patterning in leaves. *Current Topics in Developmental Biology*, **91**, 141–168.

Kim, K.W. (2019) Plant trichomes as microbial habitats and infection sites. *European Journal of Plant Pathology*, **154**(2), 157–169.

Kliebenstein, D.J., **Kroymann, J.**, **Brown, P.**, **Figuth, A.**, **Pedersen, D.**, **Gershenzon, J.** ***et al.*** (2001) Genetic control of natural variation in Arabidopsis glucosinolate accumulation. *Plant Physiology*, **126**(2), 811–825.

Kong, F. & **Yang, L.** (2023) Pathogen-triggered changes in plant development: Virulence strategies or host defense mechanism? *Frontiers in Microbiology*, **14**, 1122947.

Krasauskas, J., **Ganie, S.A.**, **Al-Husari, A.**, **Bindschedler, L.**, **Spanu, P.**, **Ito, M.** ***et al.*** (2023) Jasmonates, gibberellins, and powdery mildew modify cell cycle progression and evoke differential spatiotemporal responses along the barley leaf. *Journal of Experimental Botany*, **75**, 180–203.

Kushalappa, A.C., **Yogendra, K.N.** & **Karre, S.** (2016) Plant Innate Immune Response: Qualitative and Quantitative Resistance. *Critical Reviews in Plant Sciences*, **35**(1), 38–55.

Lacchini, E. & **Goossens, A.** (2020) Combinatorial control of plant specialized metabolism: mechanisms, functions, and consequences. *Annual Review of Cell and Developmental Biology*, **36**(1), 291–313.

Leisen, T., **Werner, J.**, **Pattar, P.**, **Safari, N.**, **Ymeri, E.**, **Sommer, F.** ***et al.*** (2022) Multiple knockout mutants reveal a high redundancy of phytotoxic compounds contributing to necrotrophic pathogenesis of *Botrytis cinerea*. *PLoS Pathogens*, **18**(3), e1010367.

Lenth, R.V. (2016) Least-squares means: the R package lsmeans. *Journal of Statistical Software*, **69**(1), 1–33.

Lew, R.R. (2019) Biomechanics of hyphal growth. In *Biology of the Fungal Cell. The Mycota vol 8* (Hoffmeister, D., and Gessler, M. eds). Cham, Switzerland: Springer International publishing, pp. 83–94.

Liñeiro, E., **Chiva, C.**, **Cantoral, J.M.**, **Sabido, E.** & **Fernández-Acero, F.J.** (2016) Phosphoproteome analysis of B. Cinerea in response to different plant-based elicitors. *Journal of Proteomics*, **139**, 84–94.

Liu, H., **Brettell, L.E.**, **Qiu, Z.** & **Singh, B.K.** (2020) Microbiome-mediated stress resistance in plants. *Trends in Plant Science*, **25**(8), 733–743.

Liu, T., **Reinhart, B.J.**, **Magnani, E.**, **Huang, T.**, **Kerstetter, R.** & **Barton, M.K.** (2012) Of blades and branches: understanding and expanding the Arabidopsis ad/abaxial regulatory network through target gene identification. *Cold Spring Harbor Symposia on Quantitative Biology*, **77**, 31–45.

Mafia, R.G., **Alfenas, A.C.**, **Ferreira, E.M.**, **Andrade, G.C.G.**, **Vanetti, C.A.** & **Binoti, D.H.B.** (2009) Effects of leaf position, surface, and entry sites on Quambalaria eucalypti infection in eucalypt. *Tropical Plant Pathology*, **34**(1), 3–9.

Malitsky, S., **Blum, E.**, **Less, H.**, **Venger, I.**, **Elbaz, M.**, **Morin, S.** ***et al.*** (2008) The transcript and metabolite networks affected by the two clades of Arabidopsis glucosinolate biosynthesis regulators. *Plant Physiology*, **148**(4), 2021–2049.

Martín-Cacheda, L., **Röder, G.**, **Abdala-Roberts, L.** & **Moreira, X.** (2024) Test of specificity in Signalling between potato plants in response to infection by Fusarium Solani and Phytophthora Infestans. *Journal of Chemical Ecology*, **2024**(6): 1–11.

Meddya, S., **Meshram, S.**, **Sarkar, D.A.-O.**, **Rakesh, S.**, **Datta, R.A.-O.**, **Singh, S.** ***et al.*** (2023) Plant stomata: an unrealized possibility in plant defense against invading pathogens and stress tolerance. *Plants*, **12**(19), 3380.

Mercier, A., **Simon, A.**, **Lapalu, N.**, **Giraud, T.**, **Bardin, M.**, **Walker, A.-S.** ***et al.*** (2021) Population genomics reveals molecular determinants of specialization to tomato in the polyphagous fungal pathogen *Botrytis cinerea* in France. *Phytopathology*, **111**(12), 2355–2366.

Miao, Z.-H., **Liu, X.** & **Lam, E.** (1994) TGA3 is a distinct member of the TGA family of bZIP transcription factors in *Arabidopsis thaliana*. *Plant Molecular Biology*, **25**(1), 1–11.

Mikkelsen, M.D., **Petersen, B.L.**, **Glawischnig, E.**, **Jensen, A.B.**, **Andreasson, E.** & **Halkier, B.A.** (2003) Modulation of CYP79 genes and glucosinolate profiles in Arabidopsis by defense signaling pathways. *Plant Physiology*, **131**(1), 298–308.

Mitreiter, S. & **Gigolashvili, T.** (2021) Regulation of glucosinolate biosynthesis. *Journal of Experimental Botany*, **72**(1), 70–91.

Naets, M., **Wang, Z.**, **Verboven, P.**, **Nicolaï, B.**, **Keulemans, W.** & **Geeraerd, A.** (2020) Size does matter—susceptibility of apple for grey mould is affected by cell size. *Plant Pathology*, **69**(1), 60–67.

Nolan, T.M. & **Shahan, R.** (2023) Resolving plant development in space and time with single-cell genomics. *Current Opinion in Plant Biology*, 2023 (9), 102444.

Pandey, D., **Rajendran, S.R.C.K.**, **Gaur, M.**, **Sajeesh, P.K.** & **Kumar, A.** (2016) Plant defense signaling and responses against necrotrophic fungal pathogens. *Journal of Plant Growth Regulation*, **35**(4), 1159–1174.

Petrasch, S., **Knapp, S.J.**, **van Kan, J.A.L.** & **Blanco, U.B.** (2019) Grey mould of strawberry, a devastating disease caused by the ubiquitous necrotrophic fungal pathogen *Botrytis cinerea*. *Molecular Plant Pathology*, **20**(6), 877–892.

Pink, H., **Talbot, A.**, **Graceson, A.**, **Graham, J.**, **Higgins, G.**, **Taylor, A.** ***et al.*** (2022) Identification of genetic loci in lettuce mediating quantitative resistance to fungal pathogens. *Theoretical and Applied Genetics*, **135**(7), 2481–2500.

Plaszkó, T., **Szűcs, Z.**, **Vasas, G.** & **Gonda, S.** (2022) Interactions of fungi with non-isothiocyanate products of the plant glucosinolate pathway: a review on product formation, antifungal activity, mode of action and biotransformation. *Phytochemistry*, **200**, 113245.

Potts, A.S. & **Hunter, M.D.** (2021) Unraveling the roles of genotype and environment in the expression of plant defense phenotypes. *Ecology and Evolution*, **11**(13), 8542–8561.

Rajniak, J., **Barco, B.**, **Clay, N.K.** & **Sattely, E.S.** (2015) A new cyanogenic metabolite in Arabidopsis required for inducible pathogen defence. *Nature*, **525**(7569), 376–379.

Rieseberg, T.P., **Dadras, A.**, **Fürst-Jansen, J.M.R.**, **Dhabalia Ashok, A.**, **Darienko, T.**, **de Vries, S.** ***et al.*** (2023) Crossroads in the evolution of plant specialized metabolism. *Seminars in Cell & Developmental Biology*, **134**, 37–58.

Ritpitakphong, U., **Falquet, L.**, **Vimoltust, A.**, **Berger, A.**, **Metraux, J.-P.** & **L'Haridon, F.** (2016) The microbiome of the leaf surface of Arabidopsis protects against a fungal pathogen. *The New Phytologist*, **210**(3), 1033–1043.

Rowe, H.C., **Walley, J.W.**, **Corwin, J.A.**, **Chan, E.K.F.**, **Dehesh, K.** & **Kliebenstein, D.J.** (2010) Deficiencies in Jasmonate-mediated plant defense reveal quantitative variation in *Botrytis cinerea* pathogenesis. *PLoS Pathogens*, **6**(4), e1000861.

Sbeiti, A.A.L., **Mazurier, M.**, **Ben, C.**, **Rickauer, M.** & **Gentzbittel, L.** (2023) Temperature increase modifies susceptibility to Verticillium wilt in Medicago spp and may contribute to the emergence of more aggressive pathogenic strains. *Frontiers in Plant Science*, **14**, 1109154.

Schäfer, M., **Pacheco, A.R.**, **Künzler, R.**, **Bortfeld-Miller, M.**, **Field, C.M.**, **Vayena, E.** ***et al.*** (2023) Metabolic interaction models recapitulate leaf microbiota ecology. *Science*, **381**(6653), eadf5121.

Schlaeppi, K., **Abou-Mansour, E.**, **Buchala, A.** & **Mauch, F.** (2010) Disease resistance of Arabidopsis to Phytophthora brassicae is established by the sequential action of indole glucosinolates and camalexin. *The Plant Journal*, **62**(5), 840–851.

Shroff, R., **Schramm, K.**, **Jeschke, V.**, **Nemes, P.**, **Vertes, A.**, **Gershenzon, J.** ***et al.*** (2015) Quantification of plant surface metabolites by matrix-assisted laser desorption-ionization mass spectrometry imaging: glucosinolates on Arabidopsis thaliana leaves. *The Plant Journal*, **81**(6), 961–972.

Siegmund, U. & **Viefhues, A.** (2016) Reactive Oxygen Species in the Botrytis – Host Interaction. In: Fillinger, S. & Elad, Y. (Eds.) *Botrytis—the Fungus, the Pathogen and its Management in Agricultural Systems*. Cham: Springer International Publishing, pp. 269–289.

Silva, C.J., **Adaskaveg, J.A.**, **Mesquida-Pesci, S.D.**, **Ortega-Salazar, I.B.**, **Pattathil, S.**, **Zhang, L.** ***et al.*** (2023) *Botrytis cinerea* infection accelerates ripening and cell wall disassembly to promote disease in tomato fruit. *Plant Physiology*, **191**(1), 575–590.

Simon, A., **Mercier, A.**, **Gladieux, P.**, **Poinssot, B.**, **Walker, A.-S.** & **Viaud, M.** (2022) *Botrytis cinerea* strains infecting grapevine and tomato display contrasted repertoires of accessory chromosomes, transposons and small RNAs. *Peer Community Journal*, **2**, e83.

Singh, R., **Caseys, C.** & **Kliebenstein, D.** (2023) Genetic and molecular landscapes of the generalist phytopathogen *Botrytis cinerea*. *Molecular Plant Pathology*, **25**(1), e13404.

Soltis, N.E., **Atwell, S.**, **Shi, G.**, **Fordyce, R.**, **Gwinner, R.**, **Gao, D.** ***et al.*** (2019) Crop domestication and pathogen virulence: interactions of tomato and *botrytis* genetic diversity. *The Plant Cell*, **31**(2), 502–519.

Soltis, P.S. & **Soltis, D.E.** (2004) The origin and diversification of angiosperms. *American Journal of Botany*, **91**(10), 1614–1626.

Sonderby, I.E., **Burow, M.**, **Rowe, H.C.**, **Kliebenstein, D.J.** & **Halkier, B.A.** (2010) A complex interplay of three R2R3 MYB transcription factors determines the profile of aliphatic Glucosinolates in Arabidopsis. *Plant Physiology*, **153**(1), 348–363.

Sønderby, I.E., **Hansen, B.G.**, **Bjarnholt, N.**, **Ticconi, C.**, **Halkier, B.A.** & **Kliebenstein, D.J.** (2007) A systems biology approach identifies a R2R3 MYB gene subfamily with distinct and overlapping functions in regulation of aliphatic glucosinolates. *PLoS One*, **2**(12), e1322.

Tang, B., **Feng, L.**, **Ding, P.** & **Ma, W.** (2023) Cell type-specific responses to fungal infection in plants revealed by single-cell transcriptomics. *Cell Host & Microbe*, **31**(10), 1732–1747.

Tenorio Berrío, R., **Verstaen, K.**, **Vandamme, N.**, **Pevernagie, J.**, **Achon, I.**, **Van Duyse, J.** ***et al.*** (2022) Single-cell transcriptomics sheds light on the identity and metabolism of developing leaf cells. *Plant Physiology*, **188**(2), 898–918.

Tian, C., **Wang, Y.**, **Yu, H.**, **He, J.**, **Wang, J.**, **Shi, B.** ***et al.*** (2019) A gene expression map of shoot domains reveals regulatory mechanisms. *Nature Communications*, **10**(1), 141.

Tsukaya, H. (2014) Comparative leaf development in angiosperms. *Current Opinion in Plant Biology*, **17**, 103–109.

Veloso, J. & **van Kan, J.A.L.** (2018) Many shades of Grey in botrytis–host plant interactions. *Trends in Plant Science*, **23**(7), 613–622.

Weiberg, A., **Wang, M.**, **Lin, F.-M.**, **Zhao, H.**, **Zhang, Z.**, **Kaloshian, I.** ***et al.*** (2013) Fungal small RNAs suppress plant immunity by hijacking host RNA interference pathways. *Science*, **342**(6154), 118–123.

Whitewoods, C.D. (2021) Riddled with holes: understanding air space formation in plant leaves. *Plos Biology*, **19**(12), e3001475.

Wu, Y., **Sexton, W.K.**, **Zhang, Q.**, **Bloodgood, D.**, **Wu, Y.**, **Hooks, C.** ***et al.*** (2023) Leaf abaxial immunity to powdery mildew in Arabidopsis is conferred by multiple defense mechanisms. *Journal of Experimental Botany*, **erad450**, 1465–1478.

Zhang, T., **Li, C.**, **Li, D.**, **Liu, Y.** & **Yang, X.** (2020) Roles of YABBY transcription factors in the modulation of morphogenesis, development, and phytohormone and stress responses in plants. *Journal of Plant Research*, **133**, 751–763.

Zhang, W., **Corwin, J.A.**, **Copeland, D.**, **Feusier, J.**, **Eshbaugh, R.**, **Chen, F.** ***et al.*** (2017) Plastic transcriptomes stabilize immunity to pathogen diversity: the Jasmonic acid and salicylic acid networks within the Arabidopsis/Botrytis Pathosystem. *The Plant Cell Online*, **29**(11), 2727–2752.

Zhou, N., **Tootle, T.L.**, **Tsui, F.**, **Klessig, D.F.** & **Glazebrook, J.** (1998) PAD4 functions upstream from salicylic acid to control defense responses in Arabidopsis. *Plant Cell*, **10**(6), 1021–1030.

Zipfel, C. (2008) Pattern-recognition receptors in plant innate immunity. *Current Opinion in Immunology*, **20**(1), 10–16.

Ziv, C., **Zhao, Z.**, **Gao, Y.G.** & **Xia, Y.** (2018) Multifunctional roles of plant cuticle during plant-pathogen interactions. *Frontiers in Plant Science*, **9**, 1088.

Zuch, D.T., **Doyle, S.M.**, **Majda, M.**, **Smith, R.S.**, **Robert, S.** & **Torii, K.U.** (2022) Cell biology of the leaf epidermis: fate specification, morphogenesis, and coordination. *The Plant Cell*, **34**(1), 209–227.